The Cryosphere Discuss., 4, 1607–1633, 2010
www.the-cryosphere-discuss.net/4/1607/2010/
doi:10.5194/tcd-4-1607-2010

The Cryosphere Discussions

The imbalance of glaciers after disintegration of Larsen B ice shelf, Antarctic Peninsula

H. Rott[1,2], F. Müller[2], T. Nagler[2], and D. Floricioiu[3]

[1]Institute of Meteorology and Geophysics, University of Innsbruck, Innsbruck, Austria
[2]ENVEO IT, Innsbruck, Austria
[3]DLR IMF, Oberpfaffenhofen, Germany

Received: 13 August 2010 – Accepted: 17 August 2010 – Published: 6 September 2010

Correspondence to: H. Rott (helmut.rott@uibk.ac.at)

Published by Copernicus Publications on behalf of the European Geosciences Union.

Abstract

The outlet glaciers to the embayment of the Larsen B Ice Shelf started to accelerate soon after the ice shelf disintegrated in March 2002. We analyse high resolution radar images of the TerraSAR-X satellite, launched in June 2007, to map the motion of outlet glaciers in detail. The frontal velocities are used to estimate the calving fluxes for 2008/2009. As reference for pre-collapse conditions, when the glaciers were in balanced state, the ice fluxes through the same gates are computed using ice motion maps derived from interferometric data of the ERS-1/ERS-2 satellites in 1995 and 1999. The difference between the pre- and post-collapse fluxes provides an estimate on the mass imbalance. For the Larsen-B embayment the 2008 mass deficit is estimated at 5.94 ± 1.55 Gt/yr, significantly lower than previously published values. The ice flow acceleration follows a similar pattern on the various glaciers, being initiated at the calving terminus. The acceleration extends far upstream, gradually decreasing in magnitude with distance from the front. This suggests stress perturbation at the glacier front being a main factor for acceleration. So far there are no signs of slow-down indicating that dynamic thinning and frontal retreat will go on.

1 Introduction

The response of grounded glacier ice to the disintegration of ice shelves is an important topic for establishing realistic scenarios on future contributions of Antarctic ice masses to sea level rise. After disintegration of the northern sections of Larsen Ice Shelf (LIS) on the Antarctic Peninsula, the outlet glaciers previously feeding the ice shelves turned into tidewater glaciers. These new boundary conditions caused major acceleration and increase of ice export, first reported by Rott et al. (2002) for Drygalski Glacier and several other glaciers calving into the Larsen-A embayment. The time scale for reaching a new equilibrium state depends on various factors, including the geometry of the glacier bed, sliding conditions, the mass supply from upper glacier reaches, and the surface mass balance. The increased velocity on the terminus of Drygalski Glacier, for example, has been maintained to date at the same level which was reached in 1999, four years after Larsen A had disappeared (Rott et al., 2008). This is known from ice motion analysis using TerraSAR-X data acquired in 2007–2009.

The outlet glaciers at Larsen B Ice Shelf started to accelerate soon after the northern and central ice shelf sections broke away in March 2002 (Riedl et al., 2005; Rignot et al., 2004; Rott et al., 2007; Scambos et al., 2004). The ice motion data were obtained by applying image correlation techniques in repeat pass images of various satellite sensors, namely optical imagery of Landsat (Scambos et al., 2004), and radar images of Radarsat-1 (Rignot et al., 2004) and of the Advanced Synthetic Aperture Radar (ASAR) on Envisat (Rott et al., 2007). Only few measurements are available on glacier surface topography and ice thickness. Surface topography and glacier thinning were observed by the Geoscience Laser Altimeter System (GLAS) of NASA's ICESat along a few tracks crossing the glaciers (Hulbe et al., 2008; Scambos et al., 2004). On Crane Glacier ice thickness and surface elevation were measured in November 2002 by Centro de Estudios Científicos, Valdivia, Chile (CECS) in cooperation with NASA using an aircraft equipped with an ice sounding radar and an altimeter (Rignot et al., 2004; Hulbe et al., 2008). Bathymetric measurements were made in the fjord after retreat of Crane Glacier (Zgur et al., 2007).

Improved data for the analysis of surface motion of the glaciers became available after the launch of TerraSAR-X in June 2007. The satellite delivers synthetic aperture radar (SAR) images at very high resolution and 11-day repeat cycle (Werninghaus and Buckreuss, 2010). During June 2007–January 2010 more than 70 SAR images were acquired by the TerraSAR-X satellite over outlet glaciers of the North-eastern Antarctic Peninsula. We used this data set to map the post-collapse flow fields of the outlet glaciers above Larsen-A and Larsen-B in greater detail and completeness than feasible with other satellite sensors. In this paper we focus at the study of glaciers in the Larsen B embayment (Fig. 1).

TCD
4, 1607–1633, 2010

TerraSAR-X derived glacier velocities at gates near the glacier front and estimates of ice thickness are the basis for estimating the calving fluxes in 2008/2009. As ice thickness measurements are available only for Crane Glacier, the cross section at the calving gate of the other glaciers was inferred from the pre-collapse mass fluxes under the assumption of mass equilibrium conditions. For the pre-collapse period accurate ice motion data are available for 1995 and 1999, derived from interferometric repeat pass SAR (InSAR) data of the ERS-1/ERS-2 tandem mission. The stability of the ice motion in 1995–1999 suggests that the glaciers were approximately in equilibrium. These mass fluxes are used as reference for estimating the mass imbalance after acceleration.

2 Data base and methods

The flow fields for the pre-collapse state are obtained from InSAR data of the ERS-1 and ERS-2 SAR satellites acquired in 1995 and 1999 (Rack et al., 2000; Rott et al., 2002). InSAR enables accurate and detailed mapping of the surface velocity of glaciers and ice sheets, but requires temporal stability of the radar phase. InSAR data of the ERS-1/ERS-2 tandem mission show reasonable to good phase stability (coherence) on the LIS glaciers because of the short (24 h) repeat pass interval. After shutdown of ERS-1 in early 2000, only SAR systems operating at longer repeat pass intervals were available, suffering from temporal decorrelation of the radar signal due to snowfall, snow drift or surface melt.

An alternative to using InSAR for mapping ice motion is cross-correlation of templates in SAR amplitude images, also called feature tracking. This technique delivers two components of the velocity vector (slant range and azimuth). It can measure shifts at fractions of a pixel (Strozzi et al., 2002). The incoherent SAR backscatter amplitude can be employed for cross-correlation, but requires distinct and stable surface features. The technique is similar to feature tracking in optical repeat pass imagery (Scambos et al., 2004). An advantage of SAR is the regular repeat observation capability, both in terms of time interval and illumination. Image correlation is less sensitive to surface displacement than InSAR, but this can at least partly be compensated by using repeat observations over longer time intervals. Another drawback is the lack of spatial detail compared to InSAR due to the required size of the templates for obtaining stable correlation peaks. This handicap is can be largely overcome by very high resolution sensors, such as the SAR of TerraSAR-X.

For mapping glacier motion in the years 2007 to 2009 we use TerraSAR-X single-look slant-range complex (SSC) images in stripmap mode, HH polarization, with 30 km swath width (Table 1). The spatial resolution of this product is 3.3 m in azimuth and 1.2 m in slant range at 150 MHz chirp bandwidth, corresponding to 2.09 m in ground range at 35° incidence angle (Breit et al., 2010), the pixel size is 1.95 m × 0.90 m (azimuth × slant range). The repeat pass interval is 11 days. In a first processing step the images are co-registered in slant-range geometry at sub-pixel accuracy. For the LIS glaciers we use a window size of 48 × 48 pixels after 2 × 2 looks pre-filtering for template matching, corresponding to a window of 187 m × 150 m at the surface. The accuracy of the derived displacement is about 0.5 pixels. For motion analysis spanning 11 days this corresponds to an accuracy of 0.09 m/day in azimuth and 0.04 m/day in ground range.

The 2-D output of the matcher is geometrically corrected for terrain distortion and geocoded to a 5 m grid referring to the UTM 20S projection to obtain a map of horizontal ice motion. If the elevation of the surface changes during the repeat interval, this has to be taken into account when transforming the 2-D displacement to horizontal motion. At the frontal gate C1 of Crane Glacier, we account for a subsidence rate of 8 cm/day in the TerraSAR-X analysis. This results in an increase of the magnitude of the 2008 ice velocity in the centre of the transverse profile by 3% compared to the value without correction. For surface lowering of the final 5 km of Crane terminus we obtained a number of about 30 m/yr in the 2008/2009 time frame, based on an estimate of ice flux divergence due to acceleration, as explained in the next section.

TCD
4, 1607–1633, 2010

The imbalance of glaciers after disintegration of Larsen B ice shelf

H. Rott et al.

For the InSAR analysis in 1995 and 1999 ERS SAR images from one look direction (descending orbit) are available, yielding only one component of the velocity vector. The data show good coherence, so that an accuracy ≤5 mm in ground range displacement (across track) could be achieved. The flow direction at the gates of the main Larsen-B outlet glaciers varies within ±40° from the across track direction in the available SAR swathes. This causes a slight decrease in accuracy of the retrieved velocity, but the uncertainty stays within ±1 cm/day. We applied the surface parallel flow assumption to derive the velocity vector. This assumption is well justified for the pre-collapse period, when the glaciers were approximately in balanced state. For level sections of a glacier, where the surface parallel flow assumption may produce spurious results, the flow direction was deduced from flow lines clearly visible in the SAR images.

We select gates about 1 km above the 2008/2009 calving front to compute the ice flux. The location of the gates for the Larsen B glaciers is shown in TerraSAR-X images (Figs. 2 and 3). The ice flow of Hektoria, Green and Evans glaciers (H-G-E) has been the largest tributary to Larsen B Ice Shelf before collapse, covering an area of 1580 km^2. In 2003 the ice front started to retreat behind the former grounding line (Riedl et al., 2005). After major retreat the terminus of Evans Glaciers separated from Hektoria-Green glaciers in 2007. By 6 March 2008 the total loss in grounded ice area of H-G-E amounted to 139 km^2 referring to the pre-collapse grounding line (Sandner, 2010).

Whereas in 2008 the front of the H-G-E glaciers still extended across a rather wide bay, the tongues of the other glaciers were confined in narrow valleys. Crane Glacier had lost 34 km^2 of grounded ice by March 2008, with a frontal retreat of 10 km. Jorum Glacier lost 25 km^2 of grounded ice by 6 March 2008, splitting into two separate sections in 2005. In 2008 the front of the three southern, smaller glaciers (Pequod, Melville, Mapple) was still near the pre-collapse grounding line. The position of the grounding line all along Larsen-A and Larsen-B ice shelf was determined by measuring tidal flexure in ERS InSAR images of 1995 and 1999 (Rack and Rott, 2004).

The ice velocity, deduced from the satellite images, is used to determine the mass flux F through a transverse section Y across a glacier terminus:

$$F_Y = \rho_\mathrm{i} \int_0^Y [u_\mathrm{m}(y)\, H(y)]\, dy \tag{1}$$

where ρ_i is the density of ice, u_m is the mean velocity of the vertical ice column and H is the ice thickness. We use a column-average ice density $\rho_i = 900\,\mathrm{kg\,m^{-3}}$. The mean velocity can be estimated from the observed surface velocity, u_s, if the deformation velocity, u_d, is known. We applied the laminar flow approximation for ice deformation to estimate u_d and u_m (Patterson, 1994). For pre-collapse conditions the relation $u_\mathrm{m} = 0.96\, u_\mathrm{s}$ is obtained for the centre of the profile C1 on Crane Glacier. For the accelerated ice flow in 2008 the computed u_d near the glacier front is very small compared to the surface velocity, so that $u_\mathrm{m} = u_\mathrm{s}$ can be applied for calculating the calving flux after ice flow acceleration.

3 Mass fluxes of Crane Glacier

3.1 Retrieval of mass fluxes

Crane Glacier is the only glacier for which ice thickness data are available. Under the assumption of stationarity during the years 1995 to 1999 the annual net mass balance, B_n, can be estimated for this glacier, assuming that the flux through the cross section C1 equals B_n integrated over the glacier area above. According to field measurements on Larsen B before the disintegration (Rack, 2000) and the analysis of radar backscatter signatures, all the area of the ice shelf and tributary glaciers belonged to the percolation zone. The mean velocities across C1 differ only by 4% in the 1995 and 1999 interferograms, with the higher value in 1995 (Fig. 4). These observations support the assumption that the glacier was close to equilibrium during the pre-collapse period. Further backup on this assumption comes from the analysis of strain rates on Larsen B, along the central flow line downstream of the glacier, based on InSAR data of 1995 to 1999 and on field measurements in 1996 and 1997 (Rack et al., 2000). Near the grounding zone no significant temporal changes of horizontal ice flow were observed, whereas the ice flow accelerated on the ice shelf towards the front indicating ice shelf thinning.

The TerraSAR-X motion analysis shows velocities of 5.1 m/day in the centre of C1 in spring (October, November) 2008, an increase by a factor of 3.4 compared to 1995/1999 (Fig. 4). In late summer 2009 (April) the velocity was 10% higher than in late winter 2008, but in November 2009 similar values were measured as in October-November 2008. As evident from the longitudinal velocity profile (Fig. 5), the interim acceleration affected only the lowest 4 km of the terminus. This suggests that it was triggered by changes in the stress conditions near the glacier front rather than enhancement of basal sliding along the terminus due to increased melt water supply.

TerraSAR-X images provide evidence for such changes. In October and November 2008 and 2009 the fjord in front of the glacier was densely covered by a melange of fast sea ice and debris of glacier ice (Fig. 6). The melange moved with a velocity slightly higher than the glacier front. This contrasts with April 2009 when the bay was covered by a thin layer of fresh ice with very little glacier ice debris, which had been transported away by offshore winds.

The main uncertainty for computing the mass flux results from the lack of data on the basal cross section. The flight line of the CECS/NASA ice thickness profile measured along the Crane tongue in November 2002 does not follow exactly the central flow line (Hulbe et al., 2008). The line crosses profile C1 about half way between the centre of the glacier and the orographically left margin, showing the glacier bed at 630 m below and the surface at 230 m a.s.l. (above sea level). It can be assumed that the surface elevation did not change much between March 2002, the date of the ice shelf collapse, and November 2002, as at that time a small ice shelf section was still in place in front of the glacier. Further support for this assumption comes from ICESat elevation

TCD
4, 1607–1633, 2010

measurements on a profile six kilometres upstream of C1. On 23 October 2003 the elevation in the centre of the profile was 290 m (Scambos et al., 2004), corresponding to the airborne elevation measurement of November 2002 within the estimated uncertainty. The elevation difference of 60 m from the ICESat profile to C1 corresponds to an inclination of 0.01, in agreement with the available pre-collapse elevation data (Jezek et al., 1999).

For computing the mass flux in 2008 glacier thinning has to be taken into account. Scambos et al. (2004) report a thinning rate of 3.1 $\mathrm{cm\,d^{-1}}$ between 23 October 2003 and 23 February 2004 at the ICESat profile. The thinning rate increased later on due to ice flow acceleration, as known from ICESat repeat measurements in 2006 (Hulbe et al., 2008). From ice flow acceleration compared to the pre-collapse state (Fig. 5) and ice thickness we estimate the ice flux divergence for the lower 5 km of the terminus. The corresponding surface lowering amounts to about 30 $\mathrm{m\,a^{-1}}$ in 2008/2009. As this accelerated thinning rate was most likely reached sometime during the year 2004, we assume surface lowering of 140 m at C1 for the pre-collapse period until end of 2008 as basis for computing the calving flux. With this value the central part of the glacier front would have been only lightly grounded and possibly locally even floating. This is plausible considering the heavily crevassed structure of the lower terminus apparent in the TerraSAR-X images (Fig. 6). The arching crevasse pattern results from a combination of simple shear near the glacier margins and longitudinal extension in the central part (Benn et al., 2007).

In order to compute the mass flux through gate C1 it is necessary to specify the geometry of the glacier bed. The shape of the velocity profiles, showing moderate variation of velocity in the central parts (Fig. 4), suggests a U-shape or trapezoidal shape of the bed. We computed the mass flux for a trapezoid with a flat base of 1800 m width at 670 m b.s.l. (below sea level). The width at the surface before collapse was 3450 m. The corresponding glacier thickness in the central part of the cross section is 900 m in 1995/1999, and 760 m in 2008. With these values the mean slope of the flanks is 47.5 degrees. In order to check the impact of the cross section shape, we computed the fluxes also for a V-shaped profile (less probable with the observed velocities) with its central part being 400 m wide at 1000 m below sea level. This profile shape is deduced from bathymetry in front of Crane Glacier, showing a narrow trench of 1000 m depth in the centre of the fjord (Zgur et al. 2007). The fluxes through C1, computed for the two different shapes of the glacier bed, agree within 2%.

3.2 Calving fluxes and net accumulation

With these specifications for C1 the flux F_{C1} (1995/1999) = 1.095 ± 0.173 Gt a^{-1} is obtained using the average of the 1995 to 1999 surface velocities corrected for ice deformation. The uncertainty estimate takes into account an error of 5% in the column mean velocity over the gate and 15% uncertainty for the area of the cross section. This corresponds to a mean specific net accumulation B_a = 1036 ± 164 kg m^{-2} a^{-1} for the drainage area above C1. No accumulation measurements are available for any of the Larsen A and Larsen B glaciers. For the central plateau in this region accumulation estimates are highly uncertain. The nearest field measurements of accumulation on the central peninsula plateau are reported for spots 140 km south-west of Crane Glacier (accumulation rate 661 kg m^{-2} a^{-1}) and 220 km north-east (accumulation rate 2478 kg m^{-2} a^{-1}) (Turner et al., 2002). On Larsen B, downstream of the grounding line of Crane Glacier, field measurements at three spots revealed a mean accumulation rate of 375 kg m^{-2} a^{-1} (Rack, 2000).

In a previous study Rignot et al. (2004) derived for Crane Glacier in 1996 an outflow of 2.6 km^3 ice a^{-1} for a gate across the grounding line, draining an area of 1193 km^2. They specify a net accumulation of 2.5 ± 0.4 km^3 ice a^{-1}, resulting in B_a = 1886 ± 314 kg m^{-2} a^{-1} for ice density of 900 kg m^{-3}, 1.82 times the value we are reporting. The reason for this difference is unclear, as no details on the assumptions for computing the mass flux are presented except the ice velocities along the central flow line which are similar to our results derived from ERS InSAR data.

For computing the annual mass flux through C1 for 2008 we use the mean velocity of the four dates of the TerraSAR-X analysis (Fig. 4). This is based on the assumption

TCD
4, 1607–1633, 2010

that the 10% increased velocity observed in April 2009 persists through 3 months, whereas the October/November velocities are representative for 9 months of the year. Full sliding is assumed, so that the surface velocity represents the mean column velocity. With the reduced cross section area due to thinning the resulting flux is F_{C1} (2008) = 3.048 ± 0.482 Gt a^{-1}. The mass imbalance amounts to 1.953 ± 0.324 Gt a^{-1}, corresponding to a mean specific net balance of −1848 ± 306 kg m^{-2} a^{-1}. This is based on the assumption that the mean net surface mass balance did not change significantly since the late 1990s. For the period 1971–2000 the mean summer temperature at the stations of the Northern Antarctic Peninsula increased by 0.33 °C per decade (Stastna, 2010). The melt contributing area comprises only the lower section of the glacier tongue, as almost all the glacier area belongs to the percolation zone. At the station Matienzo, located close to sea level on Larsen Nunatak 100 km north-east of the Crane glacier front, a mean summer temperature of −2.7 °C has been reported for previous years (Rack, 2000; Skvarca et al., 1998). For such an environment the sum of positive air temperatures and the possible melt contribution throughout summer are rather modest. For an increase of mean summer temperature by 0.5 °C between the late 1990s and 2008, the increased melt contribution caused by temperature rise would be less than 1% of the calving flux.

The velocity along the central flow line (Fig. 5) shows the acceleration propagating far upstream. With exception of 4 km above the front, where the April 2009 velocities were slightly increased, the velocity values are rather similar along the profile for all four measurement periods between October 2008 and November 2009. The ongoing state of increased velocity all along the terminus suggests that the glacier is still far from a balanced state. Downwasting needs to continue for many years until the glacier adapts to the new boundary conditions. As the pre- to post-collapse velocity difference increases towards the front, mass continuity requires the thinning rate to be higher near the front and decreasing upstream. This will cause further retreat of the terminus as the lower sections of the glacier approach floating.

TCD
4, 1607–1633, 2010

4 Imbalance of the calving glaciers of the Larsen B embayment

Whereas for Crane Glacier the pre-collapse outflow can be estimated from observed ice velocity and cross section data, this is not possible for the other glaciers due to the lack of ice thickness measurements. We infer the net accumulation for the other glaciers by assuming the accumulation rate of Crane Glacier being representative for the region. For the glaciers flowing down from the central ice divide (Hektoria-Green glaciers, Jorum Glacier main section) we adopt the same accumulation rate as for Crane Glacier. The other glaciers listed in Table 2 flow down from ridges eastwards of the continental divide. For these glaciers we assume a 20% lower mean net accumulation in order to account for the west–east decrease of accumulation (Turner et al., 2002). This number derives from an estimated precipitation gradient of 1200 mm a^{-1} over 50 km horizontal distance from the central ice divide to the embayment. The upper boundaries of these glaciers are located about 20 km to the east of the main divide.

As for Crane Glacier, the reference value for the pre-collapse period is obtained by assuming balanced mass budgets. A trapezoidal cross section is defined for the gate of each glacier matching the geometric parameters so that the pre-collapse mass flux agrees with the estimated net accumulation. The glacier areas above the flux gates were mapped in geocoded Landsat images. Elevation data of the Antarctic Digital Data Base (Jezek et al., 1999) were used to define the ice divides on the plateau.

The pre- and post-collapse velocities were retrieved for all main glaciers of the Larsen-B embayment (Table 2). Each of the observed glaciers accelerated significantly. The pattern is similar as on Crane Glacier, with maximum acceleration at the front, gradually decreasing upstream. In a previous study it was presumed that the relatively narrow Mapple, Melville, and Pequod glaciers have not thinned because of the rather stable position of the front (Hulbe et al., 2008). Our observations show clearly that these glaciers are as well affected by stress-perturbation at the front after ice shelf break-up, resulting in more than two-fold acceleration that necessarily should cause thinning.

TCD
4, 1607–1633, 2010

Regarding seasonal variations in velocity, the individual glaciers behave differently. In April 2008 the velocities at the gates of Hektoria-Green glaciers and Evans Glacier were 10% higher than in October and November 2008. This is an indication of similar seasonal cycle as observed on Crane Glacier. In late summer 2009 large sections of Hektoria-Green glaciers calved off and the front retreated by several kilometres associated with further acceleration. The velocity and mass flux in Table 2 refer to the period previous to this event. On other glaciers no significant seasonal variations were observed in the available data set. This is shown in Fig. 7 for the cross section J1 of Jorum Glacier. In the central part the flow accelerated almost two-fold. The velocities between October/November 2008 and April 2009 differ only by 3%.

The total mass deficit in 2008 for the Larsen B glaciers is estimated at 5.94 ± 1.55 Gt/yr, corresponding to 1.77 times the net accumulation (Table 2). The total uncertainty estimate assumes 30% uncertainty of the cross section area at the calving gate for the glaciers other than Crane Glacier. The errors of the individual glaciers are summed up, because they may not be independent. The mass deficit corresponds to a mean specific net balance of $b_n = -1786\,\mathrm{kg\,m^{-2}\,a^{-1}}$. The values for individual glaciers range from $b_n = -755\,\mathrm{kg\,m^{-2}\,a^{-1}}$ (Jorum main glacier) and $b_n = -783\,\mathrm{kg\,m^{-2}\,a^{-1}}$ (Pequod Glacier) on the lower end, up to $b_n = -2237\,\mathrm{kg\,m^{-2}\,a^{-1}}$ (Hektoria-Green glaciers) and $b_n = -2424\,\mathrm{kg\,m^{-2}\,a^{-1}}$ (Evans Glacier). The smaller glaciers, being confined in narrow valleys, are less affected, whereas the Hektoria, Green and Evens glaciers show the highest losses. These glaciers still terminate in a wide bay. The ruptured crevasse pattern evident in the SAR images suggests that the terminal sections of these glaciers are close to floating condition, or may locally even float. This has been confirmed by further frontal retreat in 2009/2010 observed in a sequence of TerraSAR-X images.

It is of interest to compare the ice export across the calving gates to the mass deficit due to retreat of grounded ice. The retreat of grounded ice area for the glaciers in the Larsen B embayment up to 6 March 2008 amounted to $199\,\mathrm{km^2}$ referring to the 1995–1999 grounding line (Sandner, 2010). This ice was grounded well below sea level so that the contribution to sea level rise due to retreat of these ice masses is rather small. The mass above floating for the area between the grounding line and 2008 front (related to the pre-collapse surface topography) is estimated at 11.4 ± 4.5 Gt (Sandner, 2010). This corresponds to a mean annual contribution to see level rise of $1.9 \pm 0.75\,\mathrm{Gt\,a^{-1}}$ for March 2002–March 2008.

5 Conclusions

Six years after ice shelf break-up all observed glaciers draining in the Larsen-B embayment show similar behaviour. The ice velocity is significantly higher than in the pre-collapse state, by a factor ranging between 1.8 and 5.1 fold in the centre near the calving front. Velocity increase is observed far upstream from the glacier terminus, with the relative change in velocity decreasing with distance from the calving front. This suggests that the acceleration was triggered by stress perturbation at the glacier front propagating upstream through dynamic coupling, as observed also for Greenland outlet glaciers (Nick et al., 2009). Associated dynamic glacier thinning causes increase of gravitational driving stress, decrease of basal stress, and eventually leads to floating and frontal retreat. Seasonal variations of velocity are rather small or absent, suggesting that melt water from the glacier surface does not play a significant role for flow dynamics. The glacier fronts will further retreat, since a mass deficit is presently observed for each of the glaciers. The rate of frontal retreat will vary for each glacier, depending on the geometry of the glacier bed and the thinning rate.

The 2008 mean specific net balance $b_\mathrm{n} = -1786\,\mathrm{kg\,m^{-2}\,a^{-1}}$ ranging between $b_\mathrm{n} = -755\,\mathrm{kg\,m^{-2}\,a^{-1}}$ and $b_\mathrm{n} = -2424\,\mathrm{kg\,m^{-2}\,a^{-1}}$ for the different Larsen B glaciers is comparable to the current mass deficit of mountain glaciers in mid latitudes. The total mass deficit, estimated at $5.94 \pm 1.55\,\mathrm{Gt\,a^{-1}}$, amounts to 1.4% of the mean cryospheric contribution to sea level rise for the period 1993 to 2003 (Lemke et al., 2007).

We analyzed the flow fields and estimated the mass fluxes also for the tidewater glaciers terminating in the Larsen A and PGC embayments, using ERS-1 tandem data of October/November 1995 and TerraSAR-X data of 2007–2009. For these glaciers we

TCD
4, 1607–1633, 2010

observe a similar pattern of accelerated flow as for Larsen B. The increased velocity is maintained 15 yr after disintegration of the ice shelves, so that thinning and frontal retreat will go on for years.

Our preliminary analysis of mass fluxes, applying a similar technique as for the Larsen-B glaciers, results in a total annual mass deficit in 2008/2009 for the Larsen A and PGC glaciers that is close to the value reported for the Larsen-B glaciers. However, the uncertainty of the mass flux analysis is higher than at Larsen-B, because in October 1995 some of the glaciers had already started to accelerate after the ice shelf collapse in late January 1995. Moreover, ice thickness data have not been available to us so far. If ice thickness data from an airborne survey become available, this will help to consolidate our preliminary analysis of mass fluxes for Larsen A and PGC glaciers.

Our estimates for the mass deficit of the glaciers in the Larsen-B embayment are much lower than reported in previous publications. For 2003 the estimates of ice export for individual glaciers in the Larsen B embayment by Rignot et al. (2004, Table 3) are 4 to 6 times higher than our estimates for 2008. These large differences can hardly be interpreted as an effect of deceleration, as for the period where TerraSAR-X data are available to us (June 2007 to January 2010) we do not see any indication of decrease in flow velocity. Also, due to mass continuity such a large mass deficit would require strong thinning and larger frontal retreat than observed to date. For 2006 Rignot et al. (2008) estimate the mass deficit of the tidewater glaciers in the Larsen A and Larsen B embayments at $31 \pm 9\,\mathrm{Gt\,a^{-1}}$, more than twice our estimate.

These rather significant differences in the estimated ice export do not matter in terms of sea level rise because of the rather small glacier area on the Northern Antarctic Peninsula. However, precise data on ice flow dynamics and mass fluxes are relevant for quantifying glacier response to changes in boundary conditions. This is particular relevant for assessing processes that affect the stability of inland ice in response to ice shelf retreat.

Acknowledgements. We are grateful to Gino Casassa and Georg Kaser for helpful comments. This work was supported by the Space Application Programme (ASAP) of the Austrian Ministry of Traffic, Innovation, and Technology (BMVIT).

References

Benn, D. I., Warren, C. R., and Mottram, R. H.: Calving processes and the dynamics of calving glaciers, Earth-Sci. Rev., 82, 143–179, 2007.

Breit, H., Fritz, T., Balss, U., Lachaise, M., Niedermeier, A., and Vonavka, W.: TerraSAR-X SAR Processing and Products, IEEE T. Geosci. Remote, 48(2), 717–727, 2010.

Hulbe, C. L., Scambos, T. A., Youngberg, T., and Lamb A. K.: Patterns of glacier response to disintegration of the Larsen B ice shelf, Antarctic Peninsula, Global Planet. Change, 63, 1–8, 2008.

Jezek, K. C., Liu, H., Zhao, Z. and Li, B.: Improving a digital elevation model of Antarctica using radar remote sensing data and GIS techniques, Pol. Geogr., 23, 185–200, 1999.

Lemke, P., Ren, J., Alley, R. B., Allison, I., Carrasco, J., Flato, G., Fujii, Y., Kaser, G., Mote, P., Thomas, R. H., and Zhang, T.: Observations: changes in snow, ice and frozen ground, in: Climate Change 2007: The Physical Science Basis. Contribution of Working Group I to the Fourth Assessment Report of the Intergovernmental Panel on Climate Change, Cambridge Univ. Press, Cambridge, UK and New York, NY, USA, 337–383, 2007.

Nick, F. M., Vieli, A., Howat, I. M., and Joughin, I.: Large-scale changes in Greenland outlet glacier dynamics triggered at the terminus, Nat. Geosci., 2, 110–114, doi:10.1038/ngeo394, 2009.

Paterson, W. S. B.: The physics of glaciers, Third Edition, Oxford, Elsevier, 1994.

Rack, W.: Dynamic behaviour and disintegration of the Northern Larsen Ice Shelf, Antarctic Peninsula, Ph.D. thesis, University of Innsbruck, Austria, 166 pp., 2000.

Rack, W., Doake, C. S. M., Rott, H., Siegel, A., and Skvarca, P.: Interferometric analysis of the deformation pattern of the Northern Larsen Ice Shelf, Antarctic Peninsula, compared to field measurements and numerical modelling, Ann. Glaciol., 31, 205–210, 2000.

Rack, W. and Rott, H.: Pattern of retreat and disintegration of Larsen B ice shelf, Antarctic Peninsula, Ann. Glaciol., 39, 505–510. 2004.

Riedl, C., Rott, H., and Rack, W.: Recent variations of Larsen Ice Shelf, Antarctic Peninsula, observed by Envisat, in: Proceedings of the 2004 Envisat and ERS Symposium, Salzburg, Austria, 6–10 September 2004, ESA SP-572, 6 pp., 2005.

Rignot, E., Casassa, G., Gogineni, P., Rivera, A., and Thomas, R.: Accelerated ice discharges from the Antarctic Peninsula following the collapse of the Larsen B ice shelf, Geophys. Res. Lett., 31, L18401, doi:10.1029/2004GL020697, 2004.

Rignot, E., Bamber, J. L., van den Broeke, M. R., Davis, C., Li, Y., van de Berg, W. J., and van Meijgaard, E.: Recent Antarctic ice mass loss from radar interferometry and regional climate modelling, Nat. Geosci., 1, 106–110, doi:10.1038/ngeo102, 2008.

Rott, H., Rack, W., Skvarca, P. and De Angelis, H.: Northern Larsen Ice Shelf, Antarctica: Further retreat after collapse, Ann. Glaciol., 34, 277–282, 2002.

Rott, H., Nagler, T., and Rack, W.: Increased export of grounded ice after the collapse of Northern Larsen Ice Shelf, Antarctic Peninsula, observed by Envisat ASAR, Proceedings of IEEE Geoscience and Remote Sensing Symp, IGARSS-07, 23–27 July 2007, Barcelona, Spain, 673–675, 2007.

Rott, H., Nagler, T., Eineder, M., and Floricioiu, D.: New results on dynamic instability of Antarctic Peninsula glaciers detected by TerraSAR-X ice motion analysis, in: Proceedings of 7th EUSAR Conference 2008, Vol. 4, VDE Verlag, Berlin, Germany, 159–162, 2008.

Sandner, R.: Ice retreat after disintegration of Northern Larsen Ice Shelf, Diploma thesis, Faculty for Geo- and Atmospheric Sciences, University of Innsbruck, Austria, 97 pp., 2010.

Scambos, T., Bohlander, J. A., Shuman, C. A., and Skvarca, P.: Glacier acceleration and thinning after ice shelf collapse in the Larsen B embayment, Antarctica, Geophys. Res. Lett., 31, L18402, doi:10.1029/2004GL020670, 2004.

Skvarca, P., Rack, W., Rott, H., and Donángelo, T. I.: Evidence of recent climatic warming on the Eastern Antarctic Peninsula, Ann. Glaciol., 27, 628–632, 1998.

Stastna, V.: Spatio-temporal changes in surface air temperature in the region of the Northern Antarctic Peninsula and South Shetland islands during 1950–2003, Polar Sci., 4, 18–33, 2010.

Strozzi, T., Luckman, A., Murray, T., Wegmüller, U., and Werner, C.: Glacier motion estimation using SAR offset-tracking procedures, IEEE T. Geosci. Remote, 40, 2384–2391, 2002.

Turner, J., Lachlan-Cope, T. A., Marshall, G. J., Morris, E. M., Mulvaney, R., and Winter, W.: Spatial variability of Antarctic Peninsula net surface mass balance, J. Geophys. Res., 107(D13), 4173, doi:10.1029/2001JD000755, 2002.
Werninghaus, R. and Buckreuss, S.: The TerraSAR-X mission and system design, IEEE T. Geosci. Remote, 48(2), 606–614, 2010.
Zgur, F., Rebesco, M., Domack, E. W., Leventer, A., Brachfeld, S., and Willmot, V.: Geophysical survey of the thick, expanded sedimentary fill of the new-born Crane fjord (former Larsen B Ice Shelf, Antarctica), US Geological Survey and the National Academies; USGS OF-2007-1047, Extended Abstract 141, 2007.

TCD
4, 1607–1633, 2010

Table 1. Dates of satellite image pairs used for mapping glacier motion.

Satellite	Track/Strip	Dates
ERS-1/ERS-2	018	07-11-1995/08-11-1995
ERS-1/ERS-2	424	09-11-1999/10-11-1999
TerraSAR-X	34/09	13-10-2008/24-10-2008/04-11-2008
TerraSAR-X	34/09	07-04-2009/18-04-2009
TerraSAR-X	34/09	02-11-2009/13-11-2009
TerraSAR-X	110/05	23-03-2008/03-04-2008
TerraSAR-X	110/05	18-10-2008/29-10-2008/09-11-2008
TerraSAR-X	110/05	27-10-2009/07-11-2009/18-11-2009

TCD
4, 1607–1633, 2010

Table 2. Drainage area, velocities at the centre line of the gate (V_c), and discharge of glaciers in the Larsen-B embayment across the gates shown in Figs. 2 and 3.

Glacier	Gate	Area (km^2)	V_c (m/yr)		Discharge (Gt/yr)		
			1995/1999	2008	1995/1999	2008	Δ
Hektoria-Green	H1, H2	1091	440	1545	1.130	3.571	2.441
Evans	E1, E2	210	93	474	0.174	0.683	0.509
Punchbowl	PU1	102	65	183	0.085	.227	0.142
Jorum north	J2	56	68	146	.046	.094	0.048
Jorum main	J1	318	475	865	.329	.569	0.240
Crane	C1	1057	548	1882	1.095	3.048	1.953
Mapple	MA1	165	37	82	.137	.288	0.151
Melville	ME1	218	73	201	.181	.473	0.292
Pequod	PE1	212	66	135	.176	.342	0.166
Sum		3327			3.353	9.295	5.942

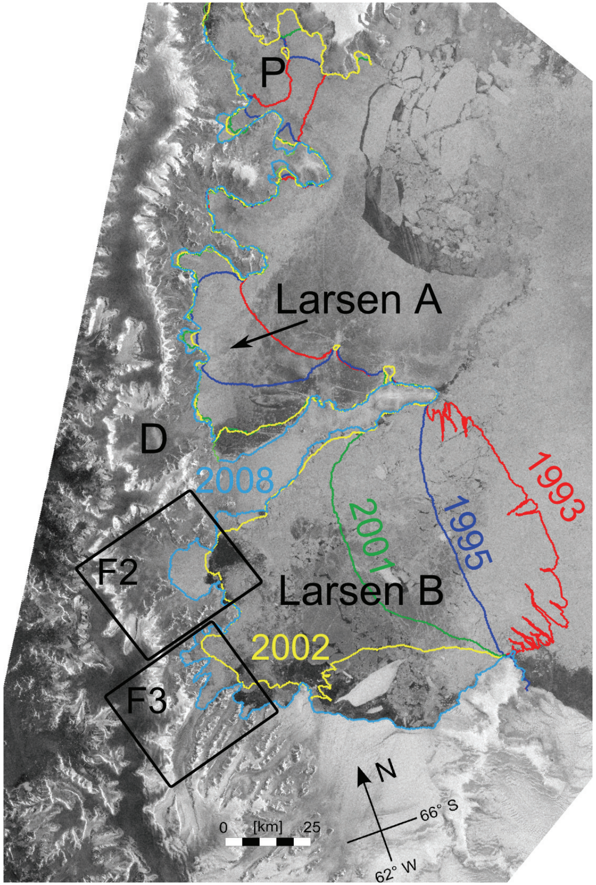

Fig. 1. Section of Envisat ASAR Wide Swath image of the Northern Larsen Ice Shelf, 6 March 2008, geocoded. P – former ice shelf in Prince Gustav Channel. Red, blue, green, yellow, cyan line: ice edge on 8 December 1992, 30 January 1995, 6 October 2000, 18 March 2002, 6 March 2008. D – Drygalski Glacier. F2, F3: location of Figs. 2, 3.

TCD
4, 1607–1633, 2010

The imbalance of glaciers after disintegration of Larsen B ice shelf

H. Rott et al.

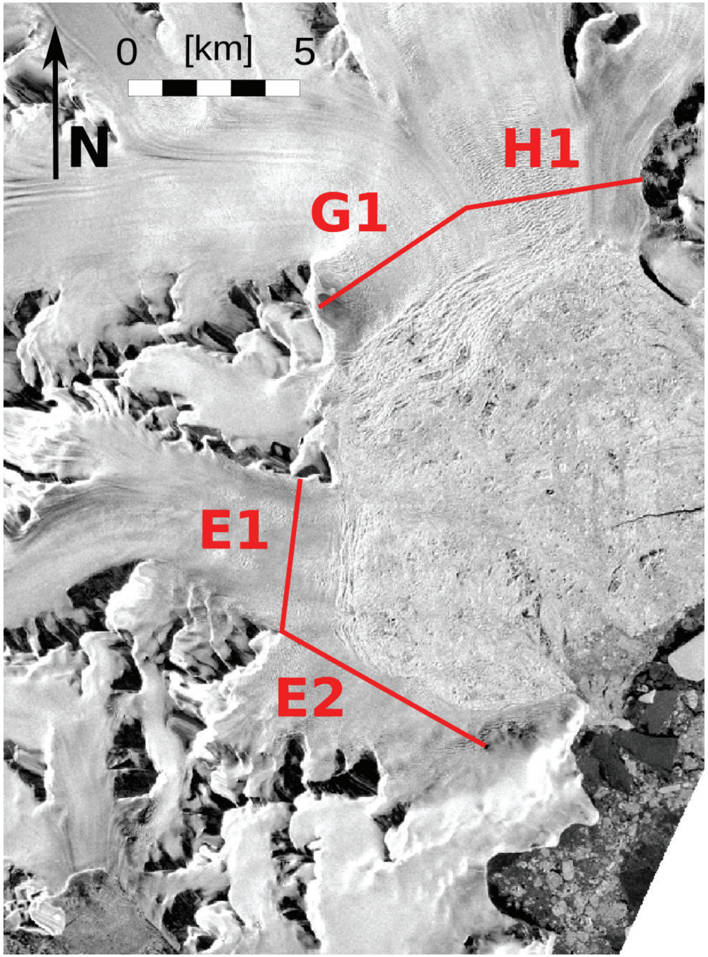

Fig. 2. TerraSAR-X image of Antarctic Peninsula glaciers draining into the Northern Larsen-B embayment, acquired 18 October 2008, with gates for mass fluxes as specified in Table 2.

TCD
4, 1607–1633, 2010

Title Page
Abstract | Introduction
Conclusions | References
Tables | Figures
◀| |▶
◀ ▶
Back | Close
Full Screen / Esc
Printer-friendly Version
Interactive Discussion

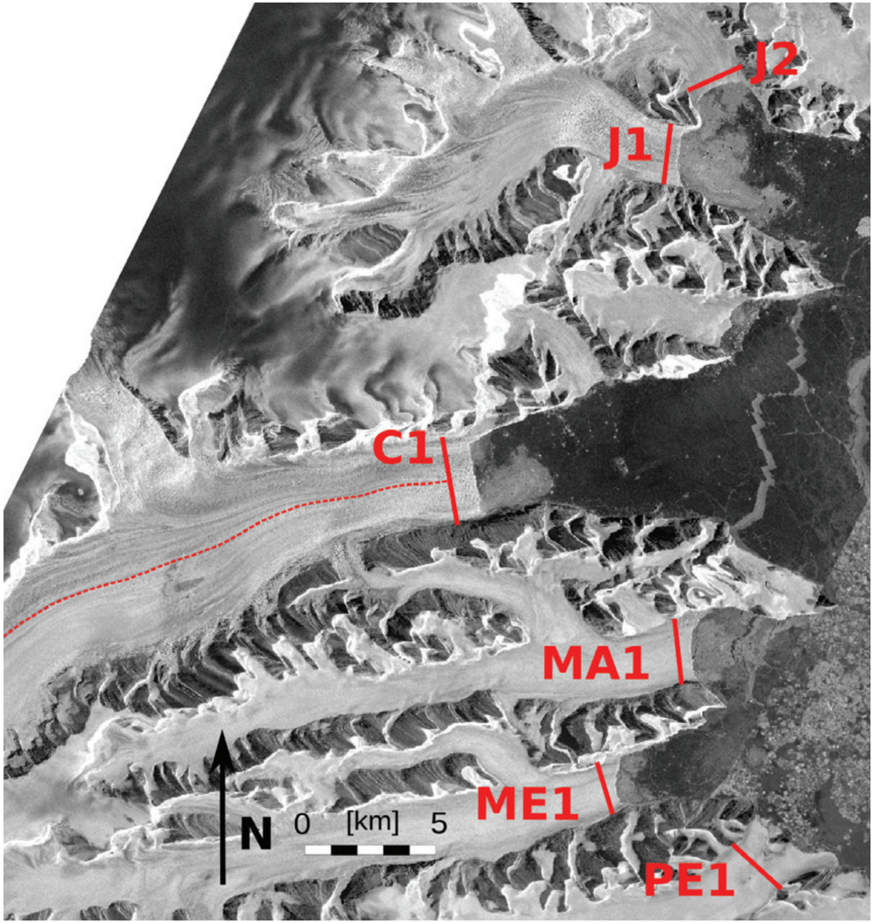

Fig. 3. As Fig. 1, covering central Larsen-B embayment, TerraSAR-X image of 7 April 2009. The gates refer to Table 2. The dotted line shows the position of the longitudinal profile of Fig. 5.

TCD
4, 1607–1633, 2010

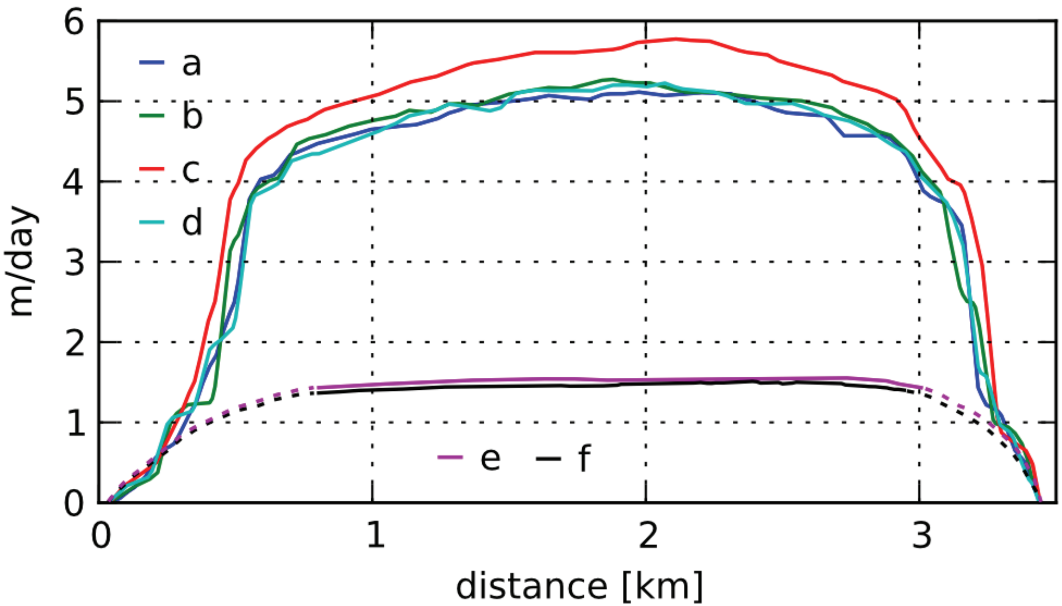

Fig. 4. Surface velocity on Crane Glacier at profile C1, derived from ERS InSAR in December 1995 **(e)** December 1999 **(f)**; from TerraSAR-X of October **(a)** and November 2008 **(b)**, April 2009 **(c)**, November 2009 **(d)**.

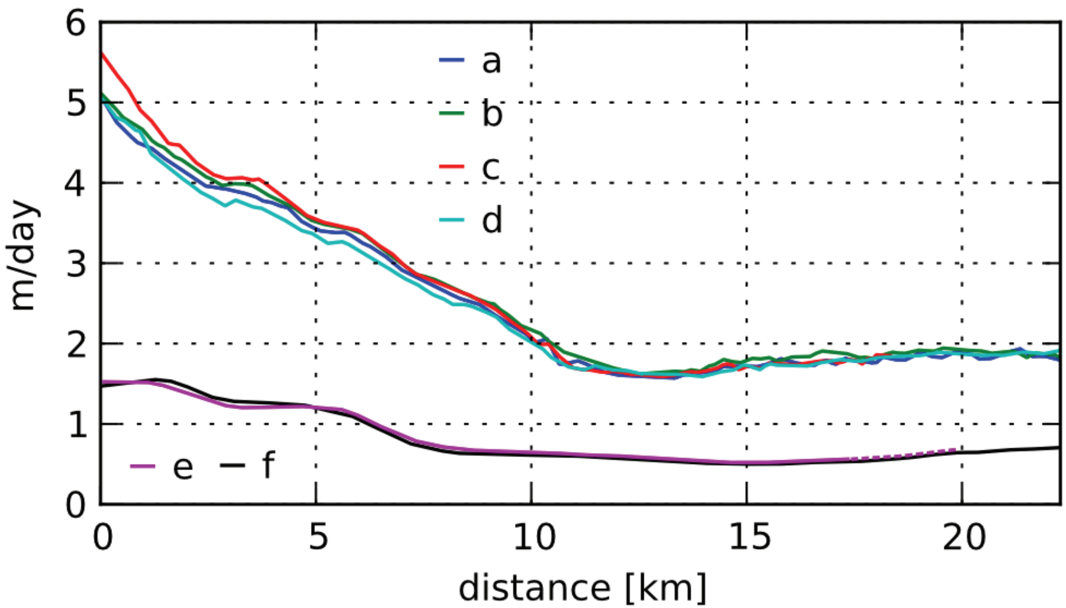

Fig. 5. As Fig. 4, profile along central flowline, starting at the centre of C1.

TCD
4, 1607–1633, 2010

The imbalance of glaciers after disintegration of Larsen B ice shelf

H. Rott et al.

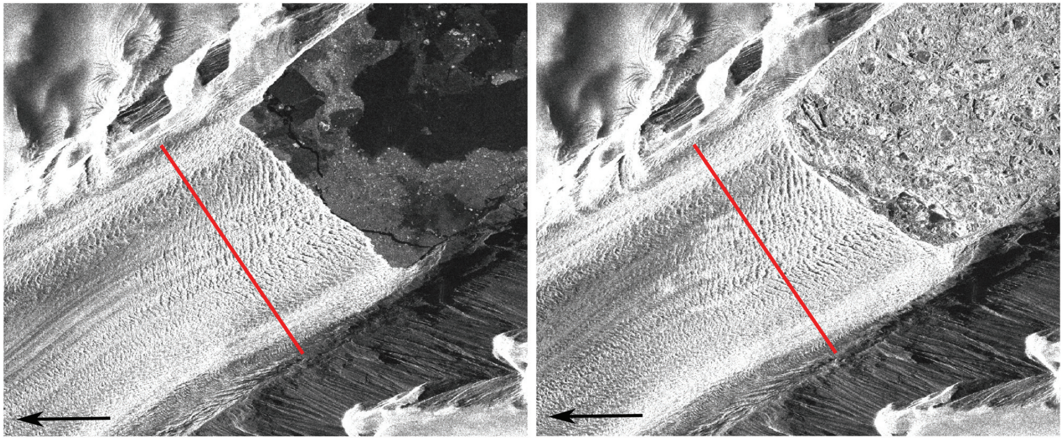

Fig. 6. Section of TerraSAR-X amplitude image of Crane Glacier terminus, 18 April 2009 (left) and 13 November 2009 (right). The arrow shows the look direction of the radar beam.

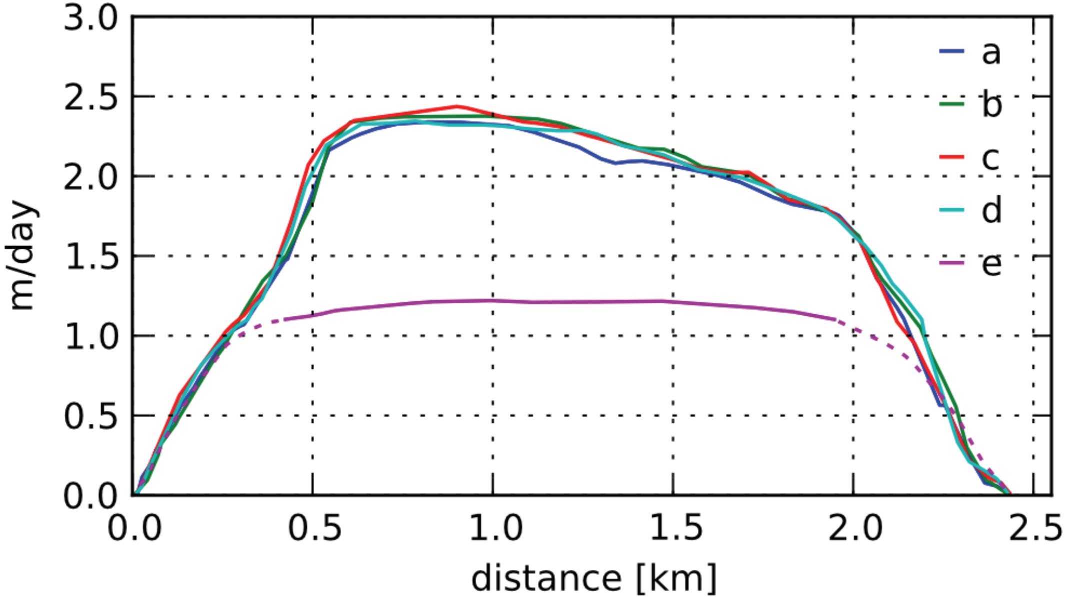

Fig. 7. Ice velocity at profile J1 on Jorum Glacier. The labels refer to the same dates as in Fig. 4.